

RESEARCH ARTICLE

EIF3D promotes resistance to 5-fluorouracil in colorectal cancer through upregulating RUVBL1

Chaobin Li¹ | Kemei Lu¹  | Chenggang Yang² | Wenfeng Du² | Zhengkai Liang²

¹Gastroenterology Department, Liaocheng People's Hospital, Liaocheng, China

²Gastrointestinal Surgery Department, Liaocheng People's Hospital, Liaocheng, China

Correspondence

Kemei Lu, Gastroenterology Department, Liaocheng People's Hospital, No. 67 Dongchang West Road, Dongchangfu District, Liaocheng City, Shandong Province, 252000, China.
Email: lukemei2009@163.com

Funding information

Shandong provincial Natural Science Foundation. Grant/Award Number: ChinaZR2015HL082

Abstract

Background: As EIF3D is oncogenic in colorectal cancer (CRC) and is associated with multidrug resistance, this study aims to investigate whether and how EIF3D regulates resistance to 5-fluorouracil (5-Fu) in CRC.

Methods: EIF3D-associated genes in CRC were predicted using bioinformatics tools. CRC cells and nude mice received 5-Fu treatment. Then, the impacts of EIF3D and the interaction between EIF3D and RUVBL1 on cell viability, colony formation, apoptosis, and DNA damage were detected through MTT, colony formation, flow cytometry, and immunofluorescence assays, and those on in vivo tumorigenesis through murine xenograft assay. IC50 value of 5-Fu for CRC cells was determined by probit regression analysis. Expressions of EIF3D, eIF4E, EIF3D-associated genes, γ H2AX, Bcl-2, Bax, and Cleaved Caspase-3/Caspase-3 in CRC tissues, cells, and/or xenograft tumors were analyzed by qRT-PCR and/or Western blot.

Results: EIF3D and RUVBL1 were highly expressed and positively correlated with CRC tissues/cells. In CRC cells, except for eIF4E, both EIF3D and RUVBL1 levels were upregulated by 5-Fu treatment; in addition to that, RUVBL1 level was downregulated by EIF3D silencing rather than eIF4E. Meanwhile, EIF3D silencing diminished IC50 value of 5-Fu and potentiated 5-Fu-induced viability decrease, colony formation inhibition, apoptosis promotion, Bcl-2 downregulation, and γ H2AX, Bax, and Cleaved Caspase-3/Caspase-3 upregulation but reversed 5-Fu-triggered RUVBL1 upregulation. RUVBL1 overexpression offsets EIF3D silencing-induced viability decrease and apoptosis promotion of 5-Fu-treated CRC cells, and tumorigenesis suppression and apoptosis promotion in 5-Fu-treated mice.

Conclusion: EIF3D promotes resistance to 5-Fu in CRC through upregulating RUVBL1 level.

KEYWORDS

colorectal cancer, EIF3D, resistance to 5-fluorouracil, RUVBL1

This is an open access article under the terms of the [Creative Commons Attribution-NonCommercial](https://creativecommons.org/licenses/by-nc/4.0/) License, which permits use, distribution and reproduction in any medium, provided the original work is properly cited and is not used for commercial purposes.

© 2023 The Authors. *Journal of Clinical Laboratory Analysis* published by Wiley Periodicals LLC.

1 | INTRODUCTION

Colorectal cancer (CRC), alternatively known as colon cancer, rectal cancer, or bowel cancer, is consequent to uncontrolled cell growth in the colorectum or the appendix.¹ Owing to older age, male gender, high fat intake, alcohol, red meat, smoking, and sedentary lifestyle,² the malignant transformation of adenomatous polyps that grow on the inner walls of the large intestine accounts for the majority of CRCs.¹ CRC remains one of the most devastating tumors, with a median 5-year survival rate of 18.5% for patients in the United States and 27.7% for those in Europe.^{3,4} These dismal prognoses are mainly attributed to metastasis and chemotherapy failure caused by the resistance to anticancer drugs.⁵

Chemotherapy is designed to completely remove cancer cells, during which any cells including both normal and cancer cells that are growing or dividing might be induced to become toxic.^{6,7} As an antineoplastic agent, 5-fluorouracil (5-Fu) has been used as adjuvant chemotherapy for CRC for more than five decades.⁶ However, 5-Fu has a relatively narrow therapeutic window, which means that cancer cells are prone to be resistant to it, leading to tumor recurrence.⁸ Apoptosis, a cellular event leading to cancer cell death, is an essential anticancer mechanism underlying chemotherapy, including 5-Fu.⁸ Resistance of CRC cells to 5-Fu can cause inhibition of apoptosis along with induction of proliferation, thus posing great obstacles to successful chemotherapy.^{8,9} Therefore, discovering a strategy to combat apoptosis inhibition caused by 5-Fu resistance is urgently needed.

Changes in cellular behaviors are fundamentally associated with protein synthesis at the translation initiation.¹⁰ Dysregulated protein synthesis contributes to cancer development.¹⁰ Eukaryotic translation initiation factors (EIFs), which mediate mRNA binding to the 40S ribosomal subunit, play a crucial role in eukaryotic protein synthesis.^{11,12} EIF3, the first identified EIFs, has 13 subunits, one of which is eukaryotic translation initiation factor 3D (EIF3D).¹³ Abnormally highly expressed EIF3D has been reported to be relevant to the occurrence and malignant progression of gallbladder cancer,¹⁴ bladder cancer,¹⁵ breast cancer,¹⁶ prostate cancer,¹⁷ non-small-cell lung cancer¹⁸ and CRC,¹⁹ and found to result in sunitinib resistance on renal cell carcinoma (RCC).²⁰ Currently, in CRC, an oncogenic role of EIF3D has been identified, while how EIF3D regulates apoptosis during chemotherapy resistance has yet to be investigated.

EIF4E is also an EIF, whose interaction with the 5' cap of mRNAs is thought to be critical for mRNA recognition required for translation initiation.^{21,22} Generally, translation specialized by EIF3 is initiated upon eIF4E binding to the 5' cap and requires the subsequent recruitment of EIF3 to an internal stem-loop structure in the 5' 3 untranslated region (UTR) of mRNAs, followed by ribosome scanning toward a start codon.²³ Nevertheless, recent evidence has demonstrated a new translation pathway, via which EIF3D initiates the specialized translation of a subset of cell proliferation mRNAs despite the inactivation of eIF4E.²⁴⁻²⁷

The objective of this study is to fathom out the drug-resistant characteristics of EIF3D in CRC and elucidate the related mechanism of action, in order to theoretically address 5-Fu resistance.

2 | MATERIALS AND METHODS

2.1 | Ethics statement

The work was started on the premise of acquiring written informed consent from all human participants. All animal experiments were conducted according to the guidelines of the China Council on Animal Care and Use.²⁸ The Ethics Committee and the Committee of Experimental Animals of Liaocheng People's Hospital approved the human and animal studies (approval number: 2020016 and 2,020,017).

2.2 | Clinical sample

CRC tissues and adjacent normal tissues were obtained from 30 CRC patients who underwent surgery at Liaocheng People's Hospital in 2020, snap-frozen in liquid nitrogen, and then stored at -80°C till further experiments.

2.3 | Bioinformatics analyses

Genes correlating with EIF3D were predicted through cBioPortal (<https://www.cbioportal.org/>). GEPIA2 (<http://gepia2.cancer-pku.cn/#index>) was utilized to predict genes differentially expressed in CRC. The mRNA targeted by EIF3D was predicted using starBase (<https://starbase.sysu.edu.cn/starbase2/>). The results of these predictions were screened out by a Venn diagram.

2.4 | Cell culture

Human CRC cells (HCT116, HCT15, SW480, SW620, and LOVO) and human normal colon cells (CCD-18Co) were purchased from American Type Culture Collection (CCL-247, CCL-225, CCL-228, CCL-227, CCL-229, and CRL-1459, ATCC). HCT15, SW480, and SW620 cells were maintained in Roswell Park Memorial Institute (RPMI)-1640 media (A4192301, ThermoFisher). HCT116, LOVO, and CCD-18Co cells were cultured in Dulbecco's modified Eagle's media (DMEM; D5030, Sigma-Aldrich). All the media were made to be complete media by the addition of 10% fetal bovine serum (FBS, F2442, Sigma-Aldrich) and 1% penicillin-streptomycin (P4333, Sigma-Aldrich). Cell culture was performed in humidified atmosphere containing 5% CO_2 at 37°C .

2.5 | Cell transfection

RuvB-like protein 1 (RUVBL1) overexpression plasmids were constructed with pcDNA3.1 vector (V79520, ThermoFisher) and the empty vector was specified as the control. Small interfering RNA targeting EIF3D (EIF3D siRNA1/2), eIF4E siRNA, and negative control (NC) siRNA were purchased from RIBOBIO (siG000008664A-1-5, siG000008664B-1-5, siB126581026-1-5, and siN0000001-1-5). After SW480 cells and LOVO cells (1×10^4 cells/well) seeded in 96-well plates were cultured to reach 80% confluence, the above plasmids alone or in combination were transfected into cells under the help of Lipofectamine 3000 transfection reagent (L3000015, ThermoFisher). Specifically, 0.2 μg of RUVBL1 overexpression plasmids was mixed with 10 μl of Opti-MEM and 0.4 μl of P3000 reagents. 0.2 μg of EIF3D siRNA1/2 and NC siRNA as well as 0.15 μl of Lipofectamine 3000 transfection reagent were mixed only with 10 μl of Opti-MEM media. The mixed plasmids and reagent were then incubated together at 37°C for 10 min (min) to obtain gene-lipid complexes. The obtained complexes were incubated with cells at 37°C for 48 h (h).

2.6 | 5-Fu treatment

SW480 cells and LOVO cells were treated with different concentrations (0, 0.5, 1, 2, 3, 4, 6, 9, 12 $\mu\text{g}/\text{ml}$) of 5-Fu (F6627, $\text{C}_4\text{H}_3\text{FN}_2\text{O}_2$, purity: $\geq 99\%$, Sigma-Aldrich) dissolved in 1 mol/L (M) NH_4OH (221,228, Sigma-Aldrich) at 37°C with 5% CO_2 for 0, 24, 48, or 72 h.^{10,29}

2.7 | Colony formation assay

After transfection with EIF3D/NC siRNA, SW480 cells and LOVO cells were trypsinized (9002-07-7, Sigma-Aldrich) and seeded in 6-well plates at a density of 1×10^2 cells/well. Then, the cells were incubated in the presence of 0, 0.5 and 1 $\mu\text{g}/\text{ml}$ of 5-Fu at 37°C with 10% of the complete media mentioned above for 14 days, with the media and 5-Fu renewed every 3 days. When colonies were visible, the media were discarded. The colonies were then washed with phosphate-buffered saline (PBS; 806,552, Sigma-Aldrich), followed by fixation in 4% paraformaldehyde (P6148, Sigma-Aldrich) for 5 min and subsequent staining with 0.1% crystal violet (C0775, Sigma-Aldrich) for 1 h. The number of stained colonies was determined under an inverted microscope (IXplore Standard; Olympus).

2.8 | Immunofluorescence assay

Assessment of cell DNA damage degree was conducted by detecting γH2AX positivity through immunofluorescence assay. In brief, after transfection with EIF3D/NC siRNA, SW480 cells and LOVO cells were cultured with 4 $\mu\text{g}/\text{ml}$ of 5-Fu in 4-well plates at a density

of 2.5×10^4 cells/well. The cells were then fixed by 4% paraformaldehyde for 10 min, permeabilized by 0.3% Triton X-100 (X100, Sigma-Aldrich), and blocked in 5% bovine serum albumin (BSA; A1933, Sigma-Aldrich). Later, the primary antibody against γH2AX (ab2893, 1 $\mu\text{g}/\text{ml}$, Abcam) was used to incubate the cells at 4°C overnight in the dark. After being washed with PBS, the cells were cultivated with Alexa Fluor 488-conjugated secondary antibody Goat anti-rabbit IgG (ab150077, 1: 200, Abcam) for 1 h in the dark. 4',6-diamidino-2-phenylindole (DAPI; D9542, Sigma-Aldrich) was then applied for nucleic acid staining. γH2AX -emitted fluorescence was observed via a confocal microscope (LEXT OLS5100, Olympus) under $\times 200$ magnification. Fluorescent lesions formed by more than 10 cells were considered positive for γH2AX . In addition, the immunofluorescence assay was performed to reveal the localization of EIF3D and RUVBL1 in the SW480 cells and LOVO cells. The experimental method is similar to that described above, but different antibodies are used.

2.9 | Quantitative reverse transcription polymerase chain reaction (qRT-PCR)

Total RNAs were extracted by Trizol reagents (15,596,026, ThermoFisher) from tissues and cells transfected with EIF3D/NC siRNA or RUVBL1 overexpression plasmids/the empty vector or not. The reverse transcription of the extracted RNAs into corresponding complementary DNA (cDNA) was accomplished using a reverse transcription kit (K1622, Yaanda Biotechnology). Real-time PCR reaction was developed in a PCR detection System (CFX Connect, Bio-Rad) with the help of Light Cycler 480 SYBR Green Master (Roche Diagnostics), and the primers were presented in Table 1. The reaction was initiated as follows: 95°C for 10 min, and 40 circles of 95°C for 15 s (s) and 60°C for 1 min. The expressions of related genes were measured by the $2^{-\Delta\Delta\text{Ct}}$ method.³⁰ Glyceraldehyde 3-phosphate dehydrogenase (GAPDH) served as the internal control.

2.10 | Methyl thiazolyl tetrazolium (MTT) assay

After transfection with EIF3D/NC siRNA or co-transfection with EIF3D siRNA and RUVBL1 overexpression plasmids/the empty vector, SW480 cells and LOVO cells were cultured with 0, 3, 6, 9, and 12 $\mu\text{g}/\text{ml}$ of 5-Fu in 96-well plates at a density of 1.5×10^4 cells/well. Following 48-h incubation, 20 μl of MTT solution (M1025, Solarbio) was added into the culture media for further 4-h incubation at 37°C. Thereafter, 150 μl of dimethyl sulfoxide (D8418, Sigma-Aldrich) was added for dissolving formazan generated during the incubation. Cell viability was measured at a wavelength of 570 nm by a microplate reader (ELx808, BioTek).

Meanwhile, the 50% inhibitory concentration (IC₅₀) value of 5-Fu in SW480 cells and LOVO cells was analyzed through Probit regression analysis.

TABLE 1 Primers used in quantitative reverse transcription polymerase chain reaction for related genes.

Genes	Species	Forward	Reverse
EIF3D	Human	5'-TGACACCC GTGATC CAGGA-3'	5'-TGGTAGGG CATATCCC AAAC-3'
RUVBL1	Human	5'-AGGTGAAG AGCACTACG AAGA-3'	5'-CTACTATG ACGCCACAT GCCT-3'
EIF3B	Human	5'-GGACCCGA CCGACT TGAGA-3'	5'-TTGACCCGAA TGTGTGCTG-3'
HSPD1	Human	5'-ATGCTTCG GTTACCCAC AGTC-3'	5'-AGCCCGAG TGAGAT GAGGAG-3'
RAD54L	Human	5'-AGGCAGGT CCTGTGATG ATGA-3'	5'-TCAAAGGT TTCCGAAAA GGAGAC-3'
NTMT1	Human	5'-CGAGGTGA TAGAAGACG AGAAGC-3'	5'-CGGGAGCTGT GATGTCGAT-3'
GAPDH	Human	5'-GAGAAGGC TGGGGC TCATTT-3'	5'-AGTGATGG CATGGA CTGTGG-3'

2.11 | Flow cytometry

After transfection with EIF3D/NC siRNA or co-transfection with EIF3D siRNA and RUVBL1 overexpression plasmids/the empty vector, SW480 cells and LOVO cells were cultured with 4 $\mu\text{g}/\text{ml}$ of 5-Fu for 48 h. Then, cell apoptosis was determined using Annexin V-FITC/PI apoptosis detection kit (40302ES20, Yeasen). Briefly, the processed SW480 cells and LOVO cells were digested in EDTA-free trypsin (T2600000, Sigma-Aldrich), and centrifuged twice at 3000 \times g for 5 min each time, followed by washing with PBS. After that, the cells were resuspended in Binding Buffer to adjust the concentration to 1×10^6 cells/ml. The cell suspension (100 μl) was added with Annexin V-FITC solution (5 μl) and propidium iodide (PI) solution (10 μl), following which the incubation in the dark for 15 min was conducted. A flow cytometer (Cytotflex, Beckman Coulter) was used to measure cell apoptosis.

2.12 | Murine xenograft assay

Male BALB/c nude mice (aged 6 weeks and weighing 18–22 g) were purchased from the SLAC Laboratory Animal Co., Ltd. All animals were raised in a specific pathogen-free (SPF) environment with free access to standard rodent feed and water for 7 days under a 12 h:12 h light/dark cycle. SW480 cells, which had been transfected with EIF3D/NC siRNA or co-transfected with EIF3D siRNA and RUVBL1 overexpression plasmids/the empty vector, were suspended in PBS to reach a concentration of 5×10^6 cells/ml. Then, 0.2 ml of the cell suspension was inoculated into the mice subcutaneously via the left

armpit.³¹ Afterward, all the mice were maintained in a laminar flow hood in the SPF environment. Tumor growth was observed every 3 days after inoculation, with tumor volume and weight recorded. 6 days later, 100 μl of 5-Fu (30 mg/kg) dissolved in PBS was injected into the mice intraperitoneally every 3 days.³¹ The tumor volume was calculated based on a formula: tumor volume = $\pi \times (\text{the longest diameter} \times \text{the shortest diameter}^2) / 6$. After 3 weeks of treatment, the mice were sacrificed via spinal dislocation under anesthetization using pentobarbital sodium (P010, Sigma-Aldrich). Primary tumors were excised for Western blot analysis, immunohistochemistry, and TUNEL staining.

2.13 | Immunohistochemistry assay

Tissue samples were sectioned into 4 μm slices, followed by being dewaxed with xylene and hydrated with gradient ethanol. After blocking with 3% hydrogen peroxide and microwave antigen repair, the slices were incubated with 1% bovine serum albumin (BSA), anti-EIF3D (ab155419, 1:200, Abcam), and Cleaved Caspase-3 (#9661, 1:400, Cell Signaling Technology), as well as secondary antibody in sequence. Sections were washed thrice with PBS, followed by the addition of diaminobenzidine for 10 min. Followed by counterstaining with hematoxylin and mounted, the changes in sections were observed under a microscope.

2.14 | Western blot

Total proteins were isolated by RIPA Buffer (89,900, ThermoFisher) from SW480 cells and LOVO cells with or without transfection of EIF3D/NC siRNA or co-transfection of EIF3D siRNA and RUVBL1 overexpression plasmids/the empty vector under the treatment of 5-Fu at 0, 1, 2, and 4 $\mu\text{g}/\text{ml}$ for 48 h, as well as from 5-Fu-treated mouse-derived xenograft tumors, which were formed by SW480 cells after co-transfection with EIF3D siRNA and RUVBL1 overexpression plasmids/the empty vector. The protein concentration was determined using a BCA kit (A53227, ThermoFisher). Marker (5 μl) (PR1910, Solarbio) and the proteins (40 μg) were then loaded separately and subjected to 8%–10% SDS-PAGE gel (P0678, P0670, Beyotime), subsequent to which they were transferred onto a polyvinylidene fluoride (PVDF) membrane (P2438, Sigma-Aldrich). The membrane was blocked with 5% skim milk in Tris Buffered Saline with 1% Tween 20 (TBST; TA-125-TT, ThermoFisher) for 2 h, and then cultured with primary antibodies against EIF3D (ab155419, 64 kDa, 1:1000, Abcam), RUVBL1 (ab51500, 50 kDa, 1:100, Abcam), γ H2AX (ab2893, 17 kDa, 1:1000, Abcam), Cleaved Caspase-3 (ab2302, 17 kDa, 1:50, Abcam), Caspase-3 (ab32351, 32 kDa, 1:5000, Abcam) and Glyceraldehyde 3-phosphate dehydrogenase (GAPDH, ab181602, 36 kDa, 1:10000, Abcam) at 4°C overnight. After being washed with TBST, the membrane was incubated with a secondary antibody Goat anti-Rabbit IgG (31,460, 1:10000, ThermoFisher) or Goat anti-Mouse IgG (G-21040, 1:10000, ThermoFisher) for 1 h.

Antigen–antibody reaction was detected using an enhanced chemiluminescence reagent kit (WP20005, ThermoFisher) on an automatic gel imager (Tanon-2500, Tanon), followed by grayscale analysis using ImageJ software (1.52s version, National Institutes of Health).

2.15 | Terminal deoxynucleotidyl transferase biotin–dUTP nick end labeling (TUNEL) staining

The apoptosis in 5-Fu-treated mouse-derived xenograft tumors, which were formed as mentioned above was observed by a TUNEL Assay kit (C1090, Beyotime), as indicated by the manufacturer's protocols. In short, xenograft tumor tissues, which had been dehydrated using gradient ethanol, transparentized with xylene (534,056, Sigma-Aldrich), and embedded into paraffin (1.07150, Sigma-Aldrich), were dewaxed by xylene, rehydrated by gradient ethanol, and cut into 4- μ m-thick sections. The sections were treated with 20 μ g/ml proteinase K (ST532 Beyotime) diluted by Immunol Staining Wash Buffer (PO106, Beyotime) for 20 min. Postwashing with PBS, the sections were stained with 50 μ l of TUNEL assay solution at 37°C for 60 min. Counterstaining with DAPI (D9542, Sigma-Aldrich) was conducted for nucleus staining. Apoptotic fluorescence was observed by a confocal microscope (LEXT OLS5100, Olympus) under \times 400 magnification.

2.16 | Statistical analysis

All data were processed using Graphpad Prism 8.0 (GraphPad Software Inc.), and expressed as mean \pm SD of three independent experiments. Paired *t*-tests were used to analyze differences between CRC tissues and adjacent normal tissues. Differences between the other two groups were analyzed by independent *t*-tests, and among multiple groups by one-way or two-way analysis of variance, followed by the Tukey's or Dunnett's post hoc test. The correlation between EIF3D and RUVBL1 was evaluated using Pearson's and Spearman's rank correlation analyses. $p < 0.05$ was considered statistically significant.

3 | RESULTS

3.1 | EIF3D was highly expressed in CRC cells and tissues, and was repressed by 5-Fu not along with eIF4E in CRC cells

Previous studies on CRC have confirmed that EIF3D plays a carcinogenic role, with a high expression in CRC cells.^{19,32} To verify the expression pattern of EIF3D in CRC, CRC cells and tissues were subjected to qRT-PCR, after which the expression level of EIF3D was observed to be higher in CRC tissues and CRC cells (HCT116, HCT15, SW480, SW620, and LOVO) than in the para-cancerous tissues and CCD-18Co cells (Figure 1A,B, $p < 0.001$). Of note, EIF3D

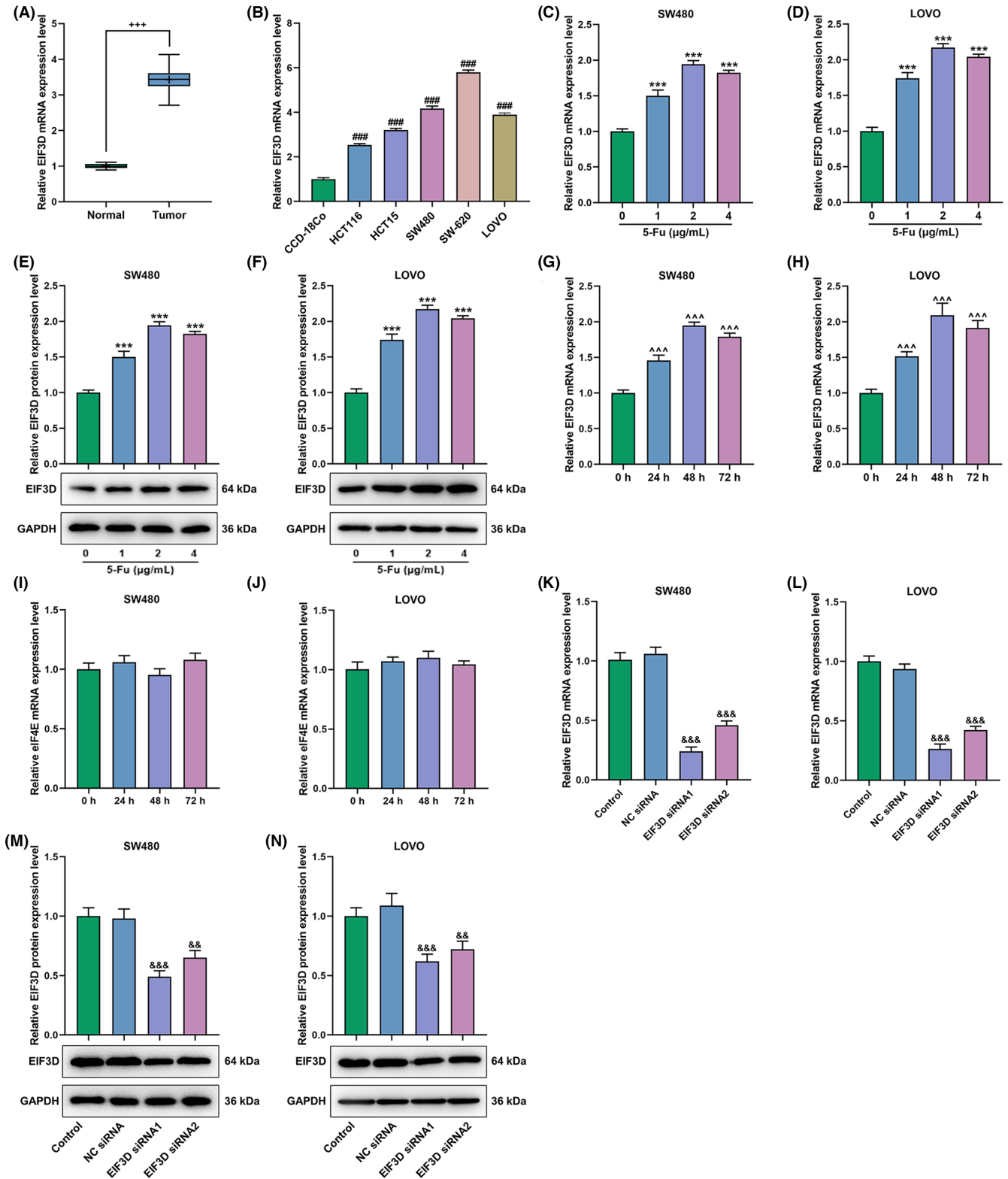
has been proposed as the culprit to induce multidrug resistance during treatment of several cancers.^{20,33} Herein, we explored whether EIF3D is associated with 5-Fu resistance in CRC. SW480 cells and LOVO cells were selected as cell models for subsequent *in vitro* experiment, as they had an average expression level of EIF3D among all the tested CRC cells. The cells were treated with 5-Fu (1, 2, and 4 μ g/ml), in which, through qRT-PCR and Western blot, EIF3D expression was discovered to be upregulated, and the upregulation was slightly more obvious under the treatment with 2 and 4 μ g/ml 5-Fu compared with the treatment with 1 μ g/ml 5-Fu (Figure 1C–F, $p < 0.001$). Though 1 μ g/ml of 5-Fu was the least efficient to upregulate EIF3D level, it did have an impact on EIF3D level and was impossible to downregulate EIF3D level. Thus, we applied 1 μ g/ml 5-Fu to treat SW480 cells and LOVO cells for a longer period of time in the following experiments conducted for investigating whether the 5-Fu-induced changes in EIF3D expression level co-occur with changes in eIF4E expression level. 1 μ g/ml 5-Fu treatment was found to be the most effective in upregulating EIF3D level at 48 h and 72 h, relative to what 5-Fu (1 μ g/ml) treatment did at 24 h (Figure 1G,H, $p < 0.001$). By contrast, no obvious change in eIF4E expression was detected at 24, 48, and 72 h in the cells after 5-Fu (1 μ g/ml) treatment (Figure 1I,J, $p < 0.001$). Furthermore, siRNAs targeting EIF3D were employed to silence EIF3D in CRC cells (SW480 and LOVO), which were then subjected to functional experiments. The results of both qRT-PCR and Western blot showed that EIF3D siRNA1 brought about a more marked silencing effect, compared with EIF3D siRNA2 (Figure 1K–N, $p < 0.01$). Thus, EIF3D siRNA1 was chosen for subsequent functional experiments conducted with various concentrations of 5-Fu.

3.2 | EIF3D silencing decreased the IC50 value of 5-Fu and strengthened 5-Fu-induced proliferation inhibition in CRC cells

Through MTT assay, we observed that EIF3D silencing potentiated 5-Fu (3, 6, 9, and 12 μ g/ml) treatment-induced concentration-dependent decrease in the viability of CRC cells (SW480 and LOVO) (Figure 2A,B, $p < 0.05$). Meanwhile, Probit regression analysis revealed that the IC50 value of 5-Fu for the cells was decreased when EIF3D was silenced in the cells (Figure 2C,D, $p < 0.05$). Moreover, 5-Fu (0.5 and 1 μ g/ml) treatment-induced promotion in CRC cell colony formation was found to be strengthened by EIF3D silencing according to the findings of colony formation assay (Figure 2E–H, $p < 0.05$).

3.3 | EIF3D silencing reinforced 5-Fu-induced apoptosis and γ H2AX positivity in CRC cells

5-Fu at 4 μ g/ml, in comparison with that at other lower concentrations, exerted a stronger anticancer effect, manifesting that alterations in CRC cell phenotypes can be observed more easily.



Hence, CRC cells (SW480 and LOVO) were treated with 4 $\mu\text{g/ml}$ 5-Fu in subsequent functional experiments. Flow cytometry-based analysis illustrated that CRC cell apoptosis was enhanced by 5-Fu treatment, which was further intensified with EIF3D silencing (Figure 3A-C, $p < 0.001$). At the same time, 5-Fu treatment decreased Bcl-2 expression, and increased the expressions

of Bax, Cleaved Caspase-3, and Cleaved Caspase-3/Caspase-3 (Figure 3D-G,I-M,O), with Caspase-3 expression remaining unchanged (Figure D,H,J,N). EIF3D silencing potentiated these 5-Fu treatment-induced effects on the above proteins except caspase-3 (Figure 3D-O, $p < 0.05$). Additionally, the immunofluorescence assay displayed that 5-Fu treatment enhanced γH2AX positivity,

FIGURE 1 EIF3D was highly expressed in CRC cells and tissues, and was repressed by 5-Fu not along with eIF4E in CRC cells. (A/B) The expression of EIF3D in CRC tissues and adjacent normal tissues (A), as well as in CCD-18Co cells, CRC cells (HCT116, HCT15, SW480, SW620, and LOVO) (B), and CRC cells (SW480 and LOVO) treated with 0, 1, 2, and 4 $\mu\text{g/ml}$ 5-Fu (C/D) was analyzed by qRT-PCR. (E/F) The expression of EIF3D in CRC cells (SW480 and LOVO) treated with 0, 1, 2, and 4 $\mu\text{g/ml}$ 5-Fu (C/D) was analyzed by Western blot, with GAPDH serving as the internal control. (G/H/I/J) The expressions of EIF3D (G/H) and eIF3E (I/J) in CRC cells (SW480 and LOVO) treated with 1 $\mu\text{g/ml}$ 5-Fu for 0, 24, 48, and 72 h were analyzed by qRT-PCR. (K/L/M/N) The expressions of EIF3D (G/H) and eIF3E (I/J) in CRC cells (SW480 and LOVO) transfected with EIF3D siRNA1/2 were analyzed by qRT-PCR (K/L) and Western blot (N/M), with GAPDH serving as the internal control. $\&\& p < 0.01$; $+++ p$, $*** p$ or $### p$ or $^^^ p$ or $\&\&\& p < 0.001$; $+$ versus Normal; $*$ versus 0 $\mu\text{g/ml}$; $\#$ versus CCD-18Co; $\hat{ }$ versus 0 h; $\hat{ }$ versus NC siRNA (CRC, colorectal cancer; 5-Fu, 5-fluorouracil; EIF3D, eukaryotic translation initiation factor 3D; EIF3D siRNA, small interfering RNA targeting EIF3D; NC, negative control; qRT-PCR, quantitative reverse transcription polymerase chain reaction; GAPDH, glyceraldehyde 3-phosphate dehydrogenase).

and this enhancing effect was strengthened by EIF3D silencing (Figure 4).

3.4 | EIF3D silencing but not eIF4E silencing decreased RUVBL1 expression in CRC cells

Bioinformatics analysis was performed with cBioPortal to predict genes correlating with EIF3D, accompanied by GEPIA2 to analyze genes differentially expressed in CRC, and starBase to predict mRNAs targeted by EIF3D. On this basis, 13 shared genes (RUVBL1, EIF3B, HSPD1, RAD54L, NTMT1, SND1, MCM7, RCC1, RANGAP1, NUP58, SLC1A5, RPS2, and MIF) were screened out using Venn diagram (Figure 5A). Among these genes, the top five were singled out for research. QRT-PCR analysis results reflected that CRC cells (SW480 and LOVO) with silent EIF3D had an obvious low expression of RUVBL1 (Figure B,C, $p < 0.001$). Notably, silencing of eIF4E left no conspicuous impact on RUVBL1 (Figure 5D,E, $p < 0.001$), suggesting that RUVBL1 was regulated by EIF3D specifically.

3.5 | RUVBL1 was highly expressed, and positively correlated with EIF3D in CRC tissues

RUVBL1 was detected to be highly expressed through qRT-PCR in CRC tissues (Figure 6A, $p < 0.001$). RUVBL1 expression was verified to positively correlate with EIF3D expression (Figure B, $p = 0.025$), which was further affirmed through cBioPortal. Analyses based on cBioPortal also uncovered a positive relation between EIF3D and RUVBL1 (Figure 6C, $p = 2.52 \times 10^{-23}$ and $p = 2.30 \times 10^{-22}$). In addition, immunofluorescence staining was performed to show the localization of EIF3D and RUVBL1 in the cells. The result showed that EIF3D was localized in the cytoplasm, and RUVBL1 was mainly localized in nucleus (Figure S1). Later, in CRC cells (SW480 and LOVO) after 5-Fu (4 $\mu\text{g/ml}$) treatment, we identified that EIF3D expression was augmented, along with up-regulated RUVBL1 and γH2AX (Figure 7A-H, $p < 0.05$). This 5-Fu (4 $\mu\text{g/ml}$) treatment-induced upregulation in the expressions of EIF3D and RUVBL1 was reversed by EIF3D silencing ($p < 0.001$), while that in γH2AX expression was magnified by EIF3D silencing (Figure 7A-H, $p < 0.05$).

3.6 | EIF3D silencing potentiated 5-Fu-induced inhibition on RUVBL1 expression and promotion on γH2AX expression in CRC cells

To ascertain the impact exerted by the interaction between RUVBL1 and EIF3D on CRC cell phenotypes, CRC cells (SW480 and LOVO) were transfected with pcDNA3.1-RUVBL1, where RUVBL1 was confirmed to be overexpressed through qRT-PCR analysis (Figure 8A,B, $p < 0.001$). EIF3D silencing-generated potentiation on 5-Fu treatment-induced decrease in CRC cell viability was proved to be offset by overexpression of RUVBL1 (Figure 8C,D, $p < 0.001$). Besides, overexpression of RUVBL1 neutralized EIF3D silencing-caused reduction in the IC50 value of 5-Fu (Figure 8E,F, $p < 0.001$). Furthermore, the enhancing effect of EIF3D silencing on 5-Fu treatment-triggered CRC cell apoptosis was reversed by RUVBL1 overexpression (Figure 8G-I, $p < 0.001$).

3.7 | RUVBL1 overexpression reversed EIF3D silencing-caused promotion on apoptosis and inhibition on tumor growth in CRC in vivo

Murine xenograft assay was conducted to unveil the impact exerted by the interaction between RUVBL1 and EIF3D in vivo on the efficiency of 5-Fu (30 mg/kg) treatment. It was found from 5-Fu (30 mg/kg)-treated mice that the volume and weight of their xenograft tumors formed by SW480 cells with silent EIF3D became smaller and lighter than those formed by the control cells (Figure 9A-C, $p < 0.001$). However, RUVBL1 overexpression drastically weakened this tumor growth suppression caused by EIF3D silencing (Figure 9A-C, $p < 0.001$). The expressions of EIF3D and Cleaved Capase-3 in xenograft tumors tissues were detected by immunohistochemistry, and the result showed that EIF3D silencing decreased the expression of EIF3D but increased the expression of Cleaved Capase-3, while RUVBL1 overexpression reversed the effect of EIF3D silencing on the Cleaved Capase-3 expression (Figure 9D,E). In the meantime, the xenograft tumors formed by SW480 cells with silent EIF3D had downregulation of EIF3D and RUVBL1, as well as upregulation of γH2AX and Cleaved Capase-3, in comparison with the xenograft tumors formed by the control cells (Figure 10A-E, $p < 0.001$). Nevertheless, when RUVBL1 was overexpressed, the

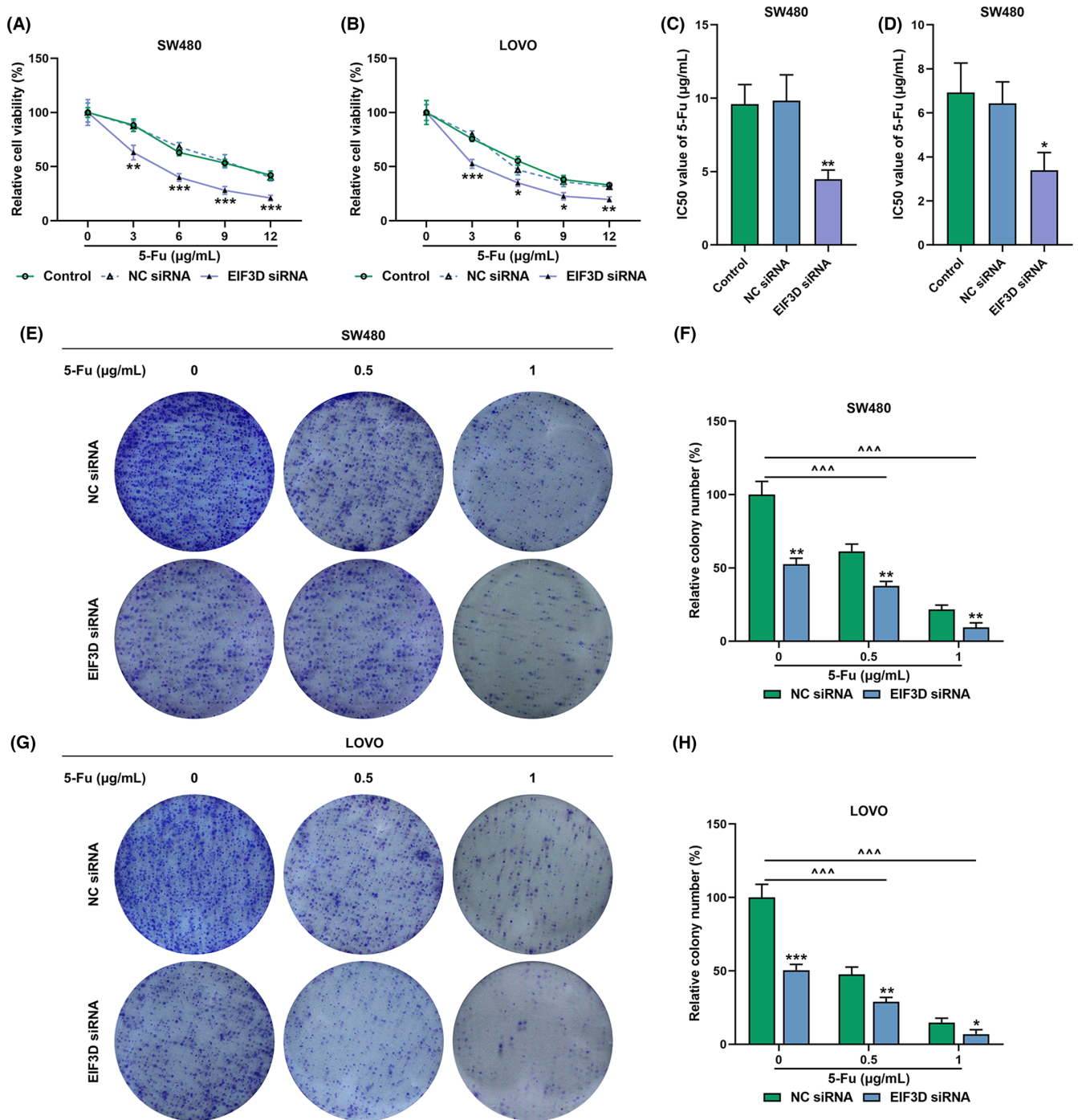


FIGURE 2 EIF3D silencing decreased the IC₅₀ value of 5-Fu and strengthened 5-Fu-induced proliferation inhibition in CRC cells. (A/B/C/D) The viability of CRC cells (SW480 and LOVO) transfected with EIF3D siRNA in the presence of 0, 3, 6, 9, and 12 µg/ml 5-Fu was measured by MTT assay (A/B), followed by determination of IC₅₀ value of 5-Fu for CRC cells through Probit regression analysis (C/D). (E/F/G/H) The colony formation of CRC cells (SW480 and LOVO) transfected with EIF3D siRNA in the presence of 0, 0.5, and 1 µg/ml 5-Fu was assessed by colony formation assay. **p* < 0.05; ***p* < 0.01; ****p* or [^]*p* < 0.001; * versus NC siRNA; [^] versus 0 µg/ml (CRC, colorectal cancer; 5-Fu, 5-fluorouracil; EIF3D, eukaryotic translation initiation factor 3D; EIF3D siRNA, small interfering RNA targeting EIF3D; NC, negative control).

EIF3D silencing-triggered trends of the expression levels of RUVBL1, γH2AX, and cleaved Capase-3 were starkly reversed (Figure 10A,C–E, *p* < 0.01), while the EIF3D silencing-caused decrease in EIF3D expression level had no significant change (Figure 10B). Also, TUNEL

assay results revealed that EIF3D silencing intensified apoptosis in SW480 cell-formed xenograft tumors of 5-Fu-treated mice, but this intensification was neutralized after RUVBL1 overexpression (Figure 10F).

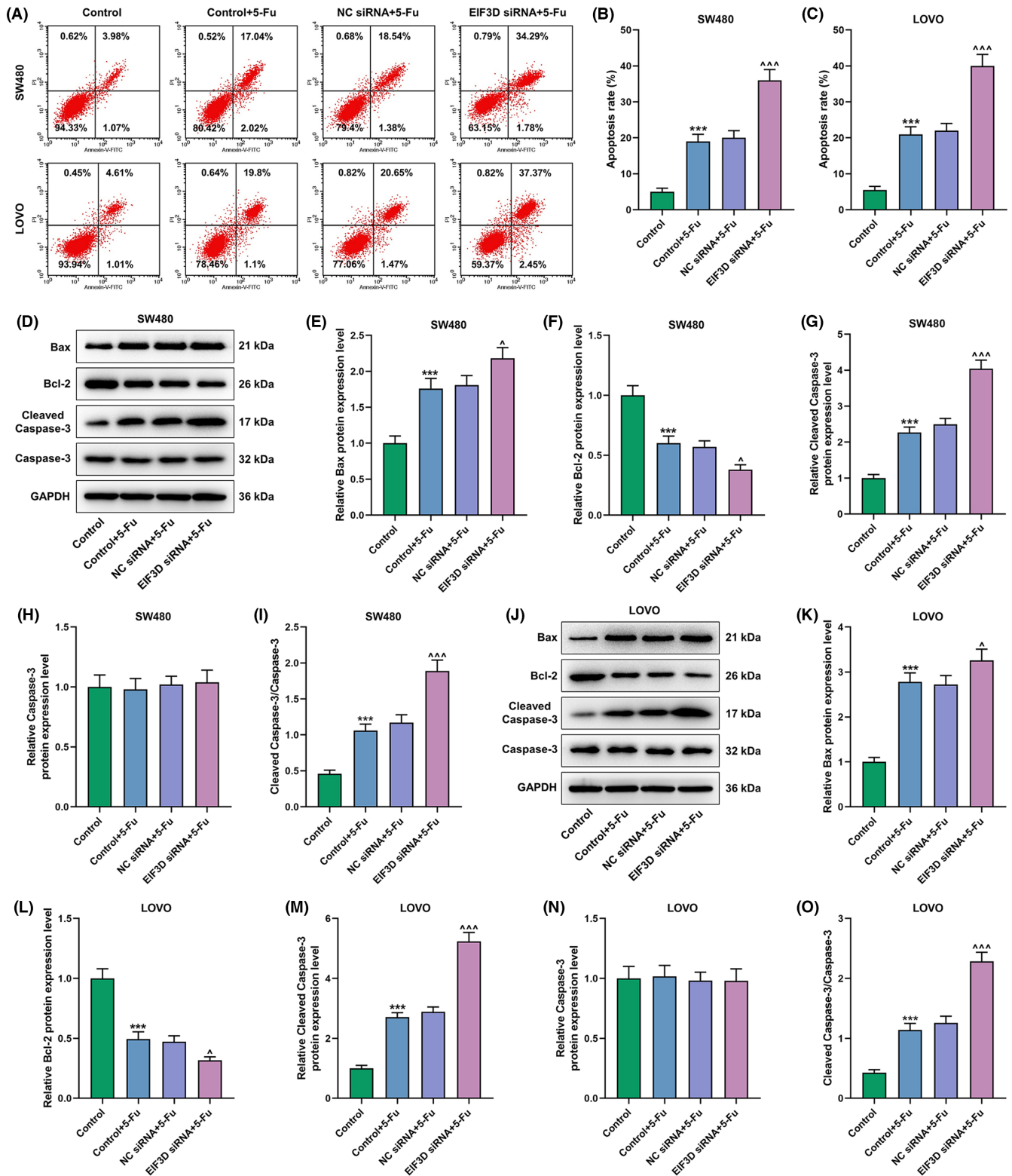


FIGURE 3 EIF3D silencing potentiated 5-Fu-induced apoptosis and γ H2AX positivity in CRC cells. (A/B/C) The apoptosis of CRC cells (SW480 and LOVO) transfected with EIF3D siRNA in the presence of 4 μ g/ml 5-Fu was measured by flow cytometry. (A/B/C/D/E/F/G/H/I/J) (D/E/F/G/H/I/J/K/L/M/N/O). The expressions of Bax, Bcl-2, Cleaved Caspase-3, Caspase-3, and Cleaved Caspase-3/Caspase-3 in CRC cells (SW480 and LOVO) transfected with EIF3D siRNA in the presence of 4 μ g/ml 5-Fu were analyzed by Western blot, with GAPDH serving as the normalizer. $^{\wedge}p < 0.05$; $^{***}p < 0.001$; $^{\wedge}$ versus Control; $^{\wedge}$ versus NC siRNA+5-Fu (CRC, colorectal cancer; 5-Fu, 5-fluorouracil; EIF3D, eukaryotic translation initiation factor 3D; EIF3D siRNA, small interfering RNA targeting EIF3D; NC, negative control; qRT-PCR, quantitative reverse transcription polymerase chain reaction; GAPDH, glyceraldehyde 3-phosphate dehydrogenase; Bcl-2, B-cell lymphoma 2; Bax, Bcl-2-associated X protein).

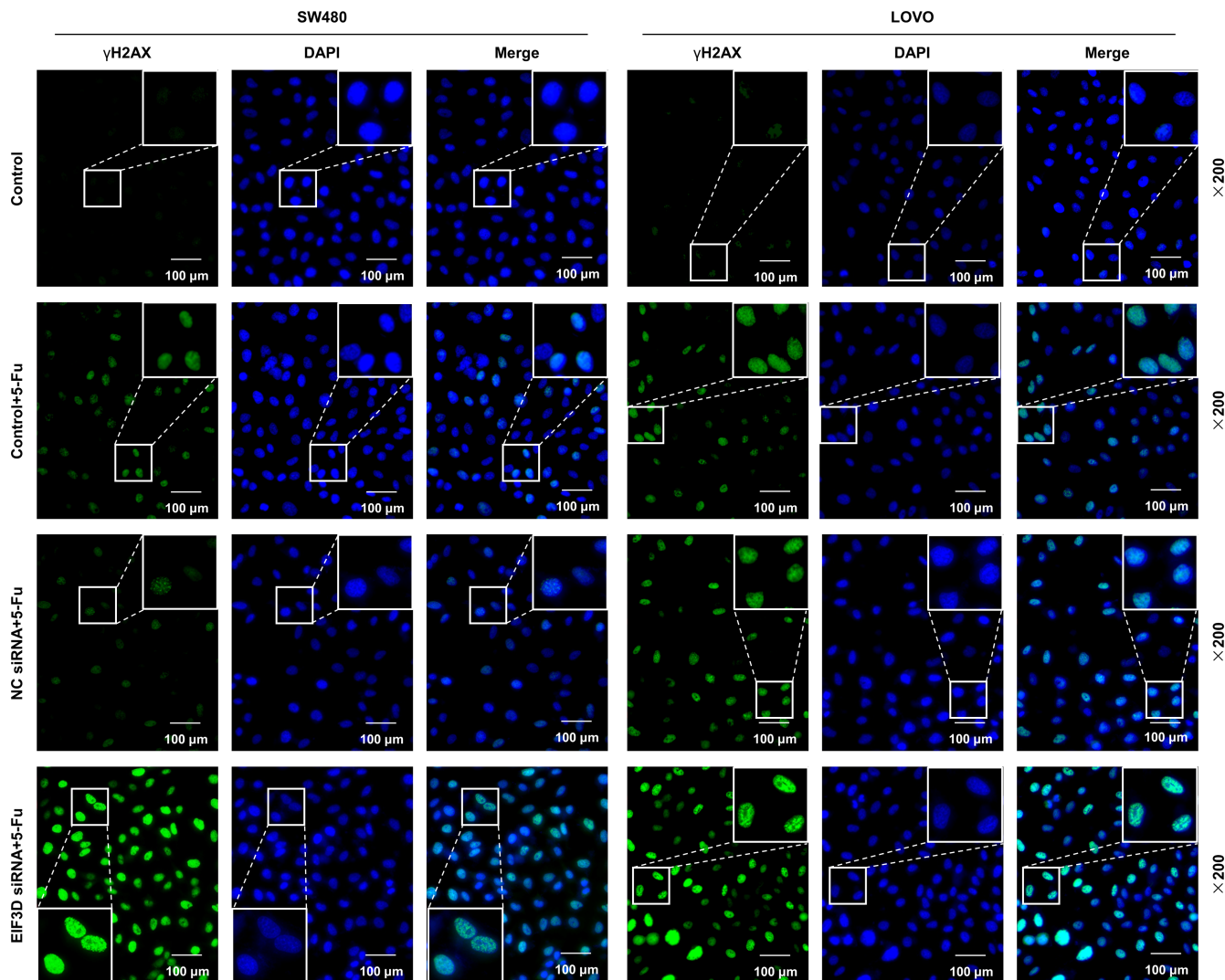


FIGURE 4 EIF3D silencing potentiated 5-Fu-induced γ H2AX positivity in CRC cells. γ H2AX positivity in CRC cells (SW480 and LOVO) transfected with EIF3D siRNA and treated with 4 μ g/ml 5-Fu was detected through immunofluorescence (magnification: $\times 200$; scale: 100 μ m) (CRC, colorectal cancer; 5-Fu, 5-fluorouracil; EIF3D, eukaryotic translation initiation factor 3D; EIF3D siRNA, small interfering RNA targeting EIF3D; NC, negative control)

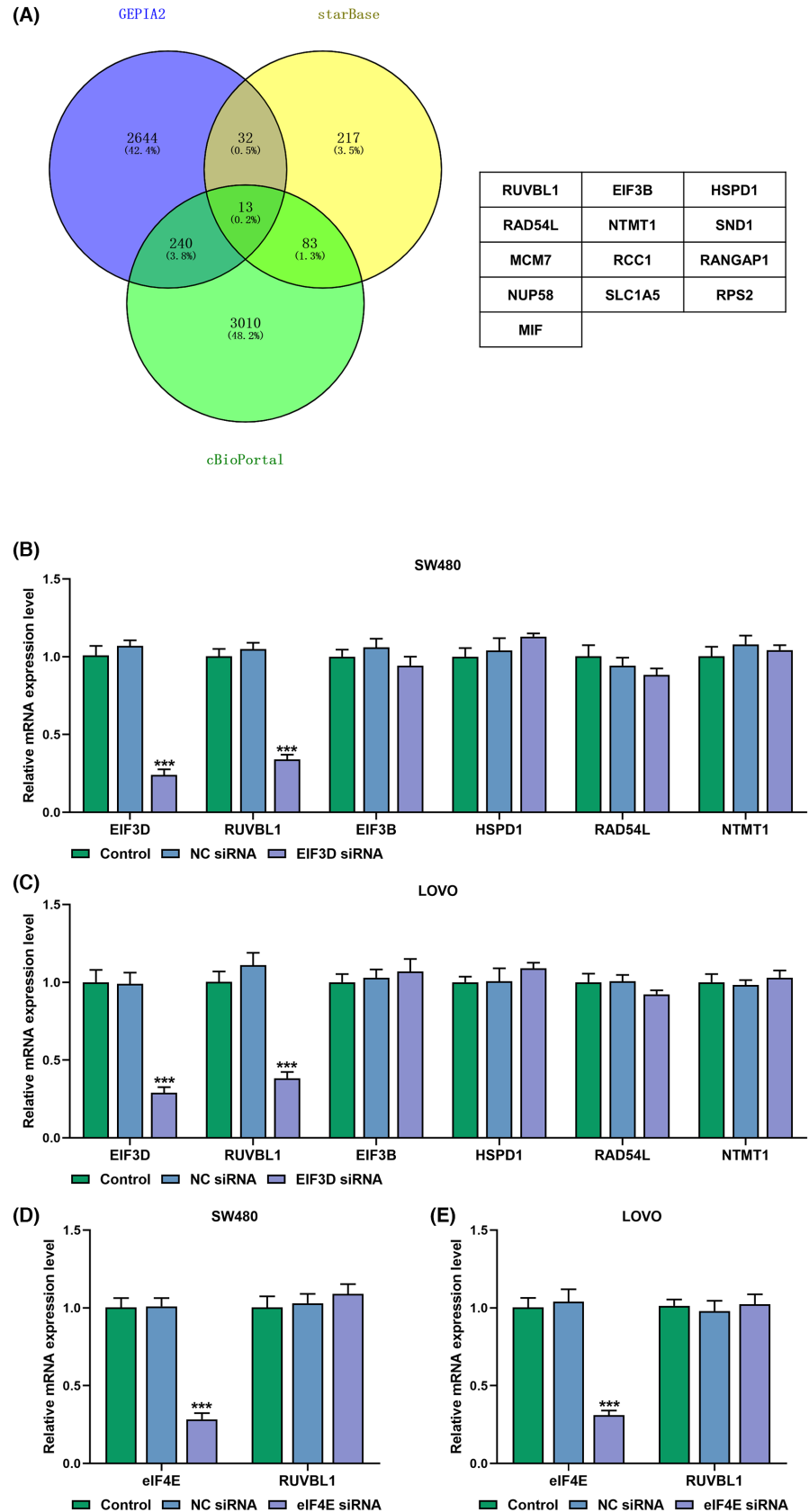
4 | DISCUSSION

The CRC prognosis worsens as the stage of the disease advances, with a decline in the 5-year survival rate of patients from 90% at stage I to barely 10% at stage IV.³⁴ Chemotherapy such as 5-Fu brings benefits to the prolongation of the survival time of patients with advanced CRC.³⁵ Unfortunately, drug resistance emerges as the deadlock of anticancer treatment, incurring disease progression.³⁴

The abundant existence of certain oncogenic proteins like WBCR22 confers drug resistance in CRC,³⁶ reflecting that the proteins have a possibility to serve as resistance biomarkers and potential targets for improving chemosensitivity. EIF3D has been identified as an oncogene highly expressed in CRC,^{19,32} which was reaffirmed by this study in both CRC tissues and cells. Studies on chemoresistance characteristics have revealed that highly

expressed EIF3D bears an association with sunitinib resistance of renal cell carcinoma (RCC)²⁰ and docetaxel resistance of prostate cancer cells.³³ 5-Fu is used as an important chemotherapeutic molecule in the current treatment of advanced CRC.³⁷ In our study, the finding of the promotive effect of 5-Fu treatment on both the mRNA and protein expressions of EIF3D, together with high expression of EIF3D in CRC as previously reported,^{19,32} suggested that EIF3D upregulation may contribute to the resistance of CRC cells against 5-Fu. 5-Fu is a synthetic fluorinated pyrimidine analog that takes effect after being intracellularly converted into active metabolites.³⁷ 5-Fu anabolism or catabolism requires the participation of enzymes like thymidylate synthase (TS), the altered action of which would trigger 5-Fu resistance.⁸ Increased mRNA expression of thymidylate synthase (TS) is related to 5-Fu resistance, and TS mRNA level is detected to be higher in 5-Fu-resistant CRC cells than in CRC cells.³⁸ We noticed that with

FIGURE 5 EIF3D silencing but not eIF4E silencing decreased RUVBL1 expression in CRC cells. (A) Genes correlating with EIF3D and differentially expressed in CRC and mRNAs targeted by EIF3D were predicted through cBioPortal, GEPIA2, and starBase, respectively, the results of which were screened out by Venn diagram. (B/C) The expressions of RUVBL1, EIF3B, HSPD1, RAD54L, and NTMT1 in CRC cells (SW480 and LOVO) transfected with EIF3D siRNA were analyzed by qRT-PCR. (D/E) The expression of RUVBL1 in CRC cells (SW480 and LOVO) transfected with eIF4E siRNA was analyzed by qRT-PCR. *** $p < 0.001$; * versus. NC siRNA (CRC, colorectal cancer; 5-Fu, 5-fluorouracil; EIF3D, eukaryotic translation initiation factor 3D; eIF4E, eukaryotic translation initiation factor 4E; EIF3D siRNA, small interfering RNA targeting EIF3D; NC, negative control; qRT-PCR, quantitative reverse transcription polymerase chain reaction; RUVBL1, RuvB-like protein 1; EIF3B, eukaryotic translation initiation factor 3B; HSPD1, heat shock protein family D (Hsp60) member 1; RAD54L, RAD54-like; NTMT1, N-terminal Xaa-Pro-Lys N-methyltransferase 1).



the prolongation of 5-Fu (1 $\mu\text{g}/\text{ml}$) treatment time, 5-Fu-induced promotion on EIF3D expression was intensified at 48 and 72 h, compared to that at 24 h, which, based on the understanding of the TS expression pattern in 5-Fu resistance, hints that CRC cells

acquire the most prominent EIF3D-related 5-Fu resistance after 48 h of treatment.

The research on sunitinib resistance in RCC has pointed out that EIF3D expression was higher in RCC cells with acquired sunitinib

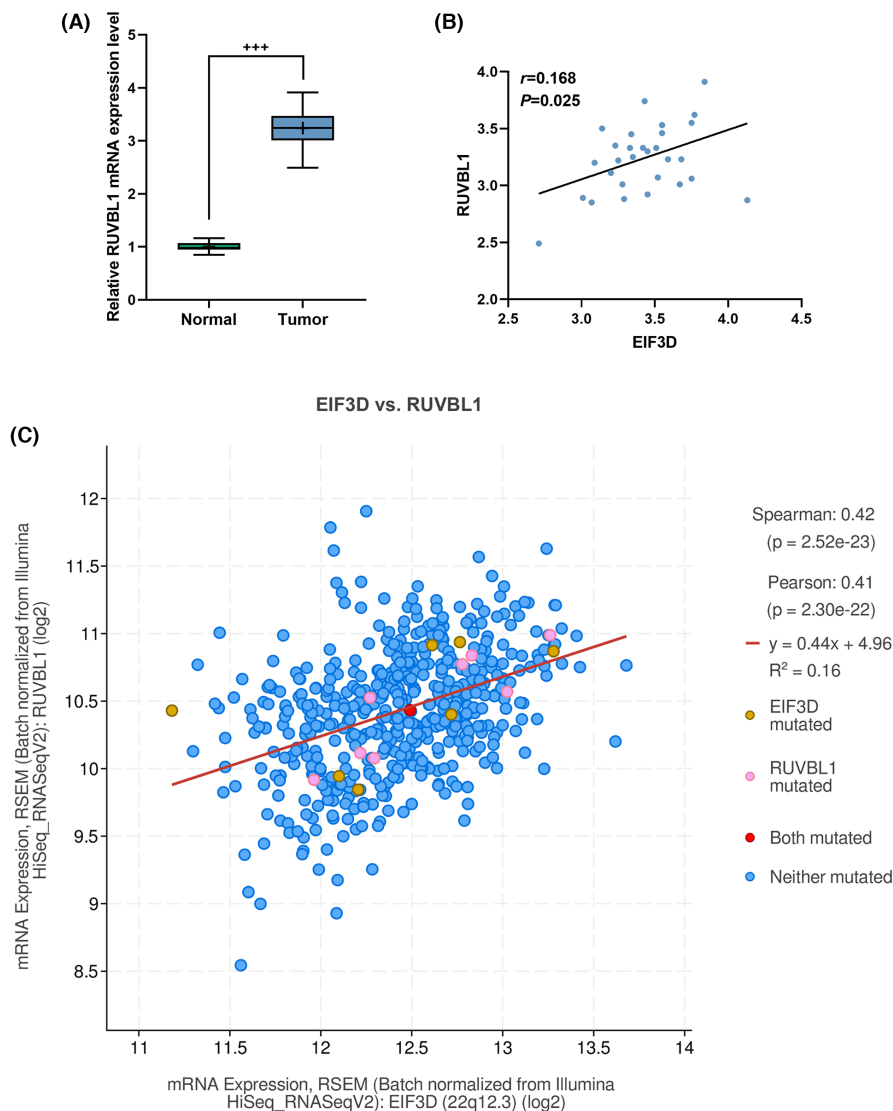


FIGURE 6 RUVBL1 was highly expressed and positively correlated with EIF3D in CRC tissues. (A) The expression of RUVBL1 in CRC tissues and adjacent normal tissues was analyzed by qRT-PCR. (B) Correlation of RUVBL1 and EIF3D in CRC tissues (C). The correlation between EIF3D and RUVBL1 was evaluated by Pearson's and Spearman's rank correlation analysis based on cBioPortal. *** $p < 0.001$; + versus Normal (CRC, colorectal cancer; 5-Fu, 5-fluorouracil; EIF3D, eukaryotic translation initiation factor 3D; qRT-PCR, quantitative reverse transcription polymerase chain reaction; RUVBL1, RuvB-like protein 1).

than in RCC cells, and knockdown of EIF3D increased the cytotoxic effect of sunitinib and reduced the IC50 value of sunitinib.²⁰ Similar to the role of EIF3D in sunitinib treatment, our study showed that EIF3D silencing potentiated 5-Fu-induced cytotoxicity, accompanied by a drop in the IC50 value of 5-Fu. Meanwhile, EIF3D is an oncogene, the knockdown of which has been recorded to inhibit CRC cell proliferation.^{19,32} Utterly, our study using colony formation assay highlighted that EIF3D silencing enhanced the anti-proliferative effect of 5-Fu in CRC cells. Furthermore, apoptosis is induced by 5-Fu to cause cell death, which indicates a decline in 5-Fu resistance.⁸ The study of Yu has discovered that CRC cell apoptosis is increased after EIF3D silencing.³² In our study, EIF3D silencing was unveiled to further strengthen the effect of 5-Fu to induce CRC cell apoptosis. Moreover, apoptosis is governed by the Bcl-2 family proteins, of which Bcl-2 inhibits apoptosis, while Bax promotes apoptosis.³⁹ Caspase-3 is the effector of the execution pathway necessary for apoptosis, the cleavage of which initiates the activation of the execution pathway that further activates cytoplasmic endonuclease and proteases to cause degradation of nuclear and cytoskeletal materials and oligonucleosomal DNA fragmentation.³⁹ We noted that

EIF3D silencing strengthened 5-Fu-induced upregulation of Bax and the conversion rate of caspase-3 into Cleaved Caspase-3, as well as downregulation of Bcl-2, which confirmed the validity of our findings pertaining to apoptosis. In addition, γ H2AX is a surrogate marker for DNA damage, and γ H2AX induction in cancer cells correlates with the suppression of tumorigenesis.⁴⁰ As anticipated, we uncovered that the number of γ H2AX-positive cells and γ H2AX protein expression were increased with 5-Fu treatment, which was further intensified by EIF3D silencing, suggesting that EIF3D silencing enhanced the ability of 5-Fu to cause CRC cell death. Taken together, our findings mirrored that EIF3D resulted in 5-Fu resistance in CRC.

EIF3, which works for translation initiation, plays a crucial role in mediating translation induction and repression.²³ The recruitment of EIF3 to the 5' UTR leads to protein synthesis, which is an important process in cancer biology.²³ As a subunit of EIF3, EIF3D is presumed to regulate protein expression, thereby affecting cancer development. This is supported by Huang's study, which has verified that EIF3D can interact with glucose-regulated protein 78 (GRP78) to block the ubiquitin-mediated proteasome degradation of GRP78, thereby causing enhanced GRP78 protein

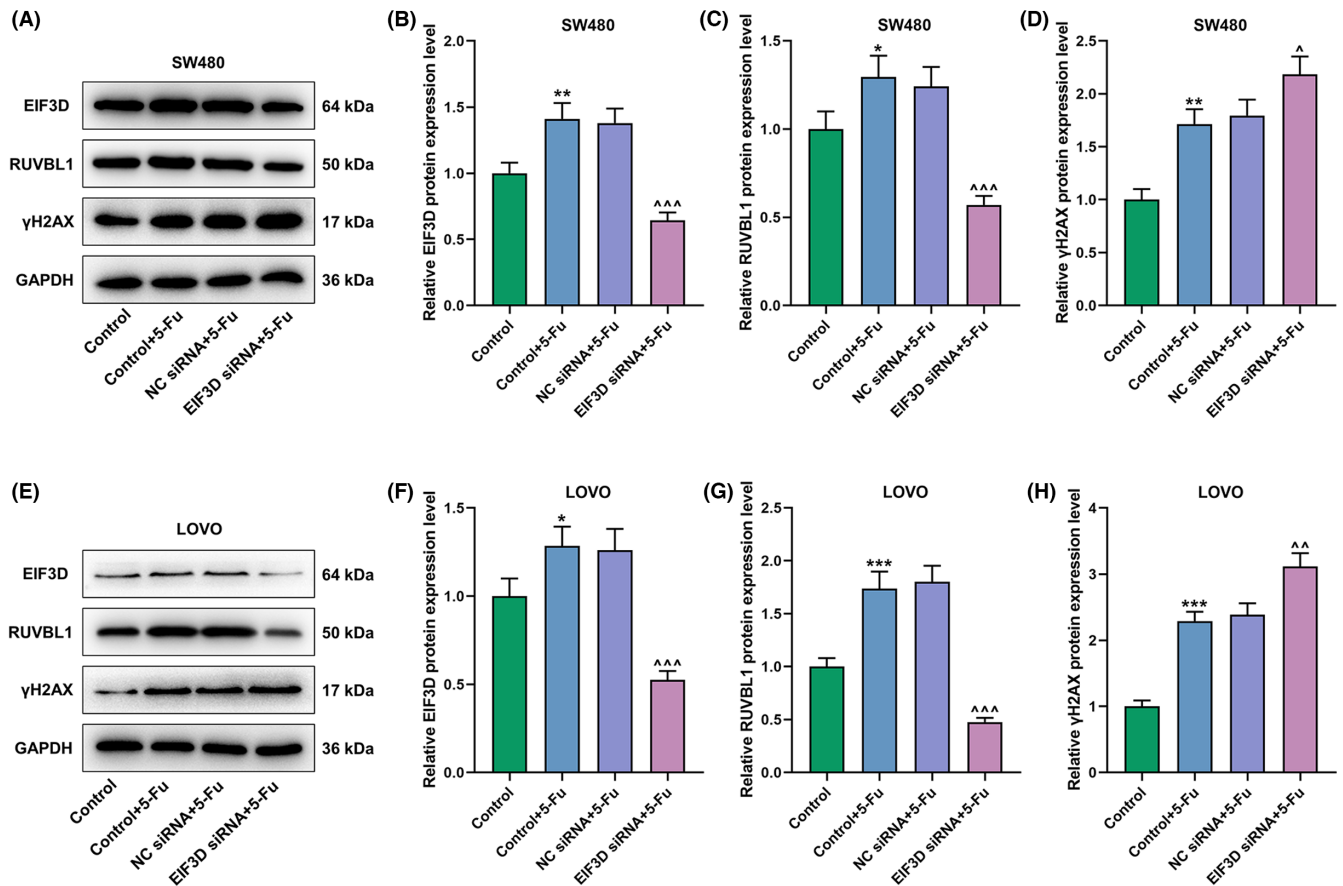


FIGURE 7 EIF3D silencing potentiated 5-Fu-induced inhibition on RUVBL1 expression and promotion on γ H2AX expression in CRC cells. (A/B/C/D/E/F/G/H) The expressions of EIF3D, RUVBL1, and γ H2AX in CRC cells (SW480 and LOVO) transfected with EIF3D siRNA and treated with 4 μ g/ml 5-Fu were analyzed by Western blot, with GAPDH serving as the internal control. * p or $\wedge p < 0.05$; ** p or $\wedge\wedge p < 0.01$; *** p or $\wedge\wedge\wedge p < 0.001$; * versus Control; \wedge versus NC siRNA+5-Fu (CRC, colorectal cancer; 5-Fu, 5-fluorouracil; EIF3D, eukaryotic translation initiation factor 3D; EIF3D siRNA, small interfering RNA targeting EIF3D; NC, negative control; qRT-PCR, quantitative reverse transcription polymerase chain reaction; RUVBL1, RuvB-like protein 1; GAPDH, glyceraldehyde 3-phosphate dehydrogenase).

stability concomitant with a stronger sunitinib resistance.²⁰ In our study, 13 CRC-associated differentially expressed mRNAs, which were correlated with EIF3D, were obtained through Venn diagram according to bioinformatics analysis. On this basis, we chose the top five most associated with EIF3D for qRT-PCR analysis. Consequently, we recognized RUVBL1 as a potential downstream mRNA of EIF3D, since RUVBL1 expression was decreased with EIF3D silencing. In a recent report, EIF3D has been demonstrated to trigger specialized translation initiation, which is distinct from general translation initiation owing to its independence on eIF4E activation.²³ Our study displayed that eIF4E expression did not change after EIF3D silencing, which, together with our findings that EIF3D increased RUVBL1 expression, confirmed that EIF3D facilitated the specialized translation of RUVBL1 to upregulate RUVBL1 level in CRC cells. Also, RUVBL1 expression has been proven to be upregulated in CRC tissues,⁴¹ as shown by our study. Moreover, we unmasked a positive correlation between RUVBL1 and EIF3D, supporting the credibility of the positive regulation of EIF3D on RUVBL1. Also known as Pontin or TIP49a, RUVBL1 is an evolutionarily conserved AAA+ protein family member with

homology to bacterial RuvB helicases and is identified as a TATA box-binding protein interacting protein.⁴² Upregulated RUVBL1 has been reported to be strongly linked to oncogenesis, which is associated with tumorigenesis and poor prognosis in various types of cancers such as breast cancer,⁴³ lung adenocarcinoma,⁴⁴ and head and neck squamous cancer.⁴⁵ Conversely, selective inhibition of the RUVBL1/2 complex can lead to cancer cell death,⁴⁶ suggesting that cell killing in drug resistance can be the consequence of RUVBL1 upregulation. In our study, 5-Fu treatment-induced RUVBL1 upregulation, which was reversed by EIF3D silencing, implying the involvement of RUVBL1 upregulation in EIF3D-caused 5-Fu resistance, and this involvement was investigated through overexpressing RUVBL1. The study of Li has discovered that RUVBL1 maintains resistance to tumor necrosis factor-related apoptosis-inducing ligand (TRAIL)-induced apoptosis in non-small-cell lung cancer.⁴⁷ Similar to this role of RUVBL1 in resistance to apoptosis, our results identified that RUVBL1 overexpression notably offsets EIF3D silencing-caused potentiation on 5-Fu-induced viability decrease and apoptosis promotion. Besides, we observed that 5-Fu treatment had no impact on eIF4E

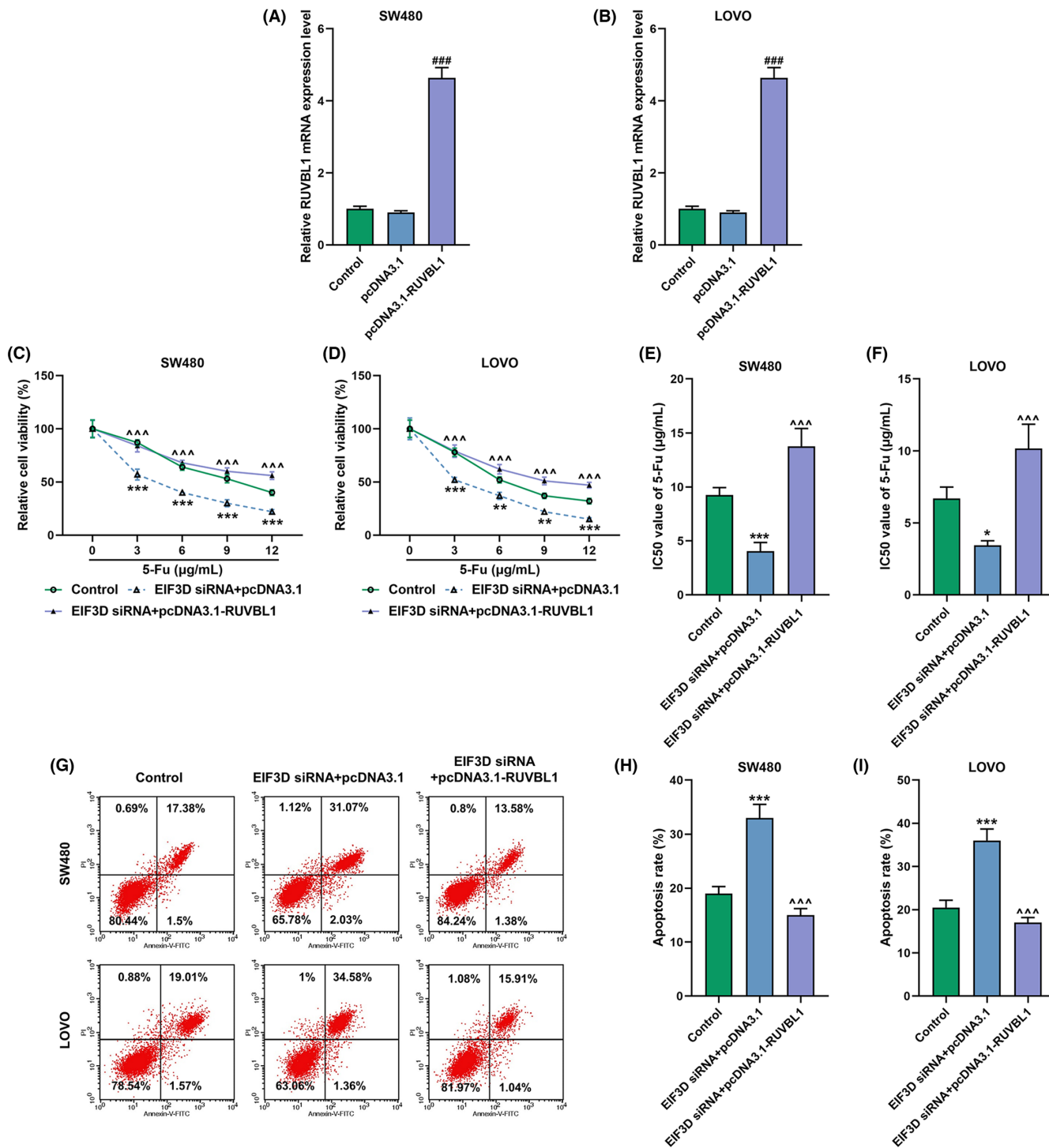
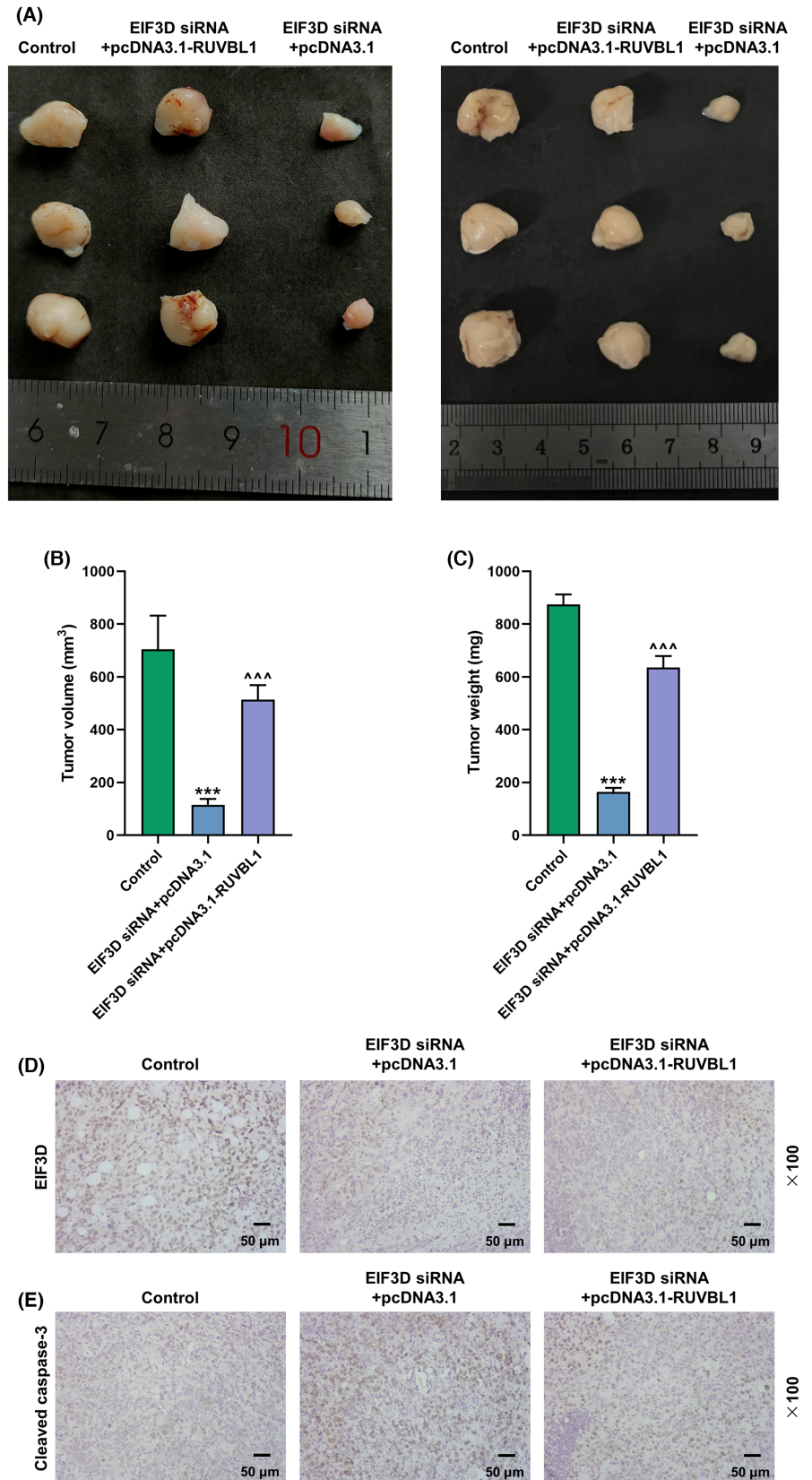


FIGURE 8 RUVBL1 overexpression reversed EIF3D silencing-caused decrease of viability and promotion of apoptosis in CRC cells. (A/B) The expression of EIF3D in CRC cells (SW480 and LOVO) transfected with RUVBL1 overexpression plasmids was analyzed by qRT-PCR. (C/D/E/F) The viability of CRC cells (SW480 and LOVO) co-transfected with EIF3D siRNA and RUVBL1 overexpression plasmids/the empty vector and treated with 0, 3, 6, 9, and 12 μg/ml 5-Fu was measured by MTT assay (C/D), followed by determination of IC50 value of 5-Fu for CRC cells through Probit regression analysis (E/F). (G/H/I) The apoptosis of CRC cells (SW480 and LOVO) co-transfected with EIF3D siRNA and RUVBL1 overexpression plasmids/the empty vector and treated with 4 μg/ml 5-Fu was measured by flow cytometry. * $p < 0.05$; ** $p < 0.01$; ### $p < 0.001$; # versus pcDNA3.1; * versus Control; ^ versus EIF3D siRNA+pcDNA3.1 (CRC, colorectal cancer; 5-Fu, 5-fluorouracil; EIF3D, eukaryotic translation initiation factor 3D; EIF3D siRNA, small interfering RNA targeting EIF3D; qRT-PCR, quantitative reverse transcription polymerase chain reaction; RUVBL1, RuvB-like protein 1; pcDNA3.1-RUVBL1, RUVBL1 overexpression plasmids).

FIGURE 9 RUVBL1 overexpression reversed EIF3D silencing-caused suppression on tumor growth in 5-Fu-treated mice. (A/B/C) In vivo tumorigenesis was assessed by murine xenograft assay in 5-Fu (30 mg/kg)-treated mice (A), with the volume (B) and weight (C) of murine xenograft tumors formed by SW480 cells co-transfected with EIF3D siRNA and RUVBL1 overexpression plasmids/the empty vector being recorded. (D/E) The expressions of EIF3D (D) and cleaved caspase-3 (E) were detected in murine xenograft tumors by immunohistochemistry. *** p or $^{^^}$ $p < 0.001$; * versus Control; * versus EIF3D siRNA+pcDNA3.1 (CRC, colorectal cancer; 5-Fu, 5-fluorouracil; EIF3D, eukaryotic translation initiation factor 3D; EIF3D siRNA, small interfering RNA targeting EIF3D; RUVBL1, RuvB-like protein 1; pcDNA3.1-RUVBL1, RUVBL1 overexpression plasmids).



expression. These findings from our study collectively indicated that EIF3D facilitated the specialized translation of RUVBL1 to trigger 5-Fu resistance.

The impact of the interaction between EIF3D and RUVBL1 on 5-Fu resistance was further proven to be potent through our murine xenograft assay. The assay results corroborated that EIF3D

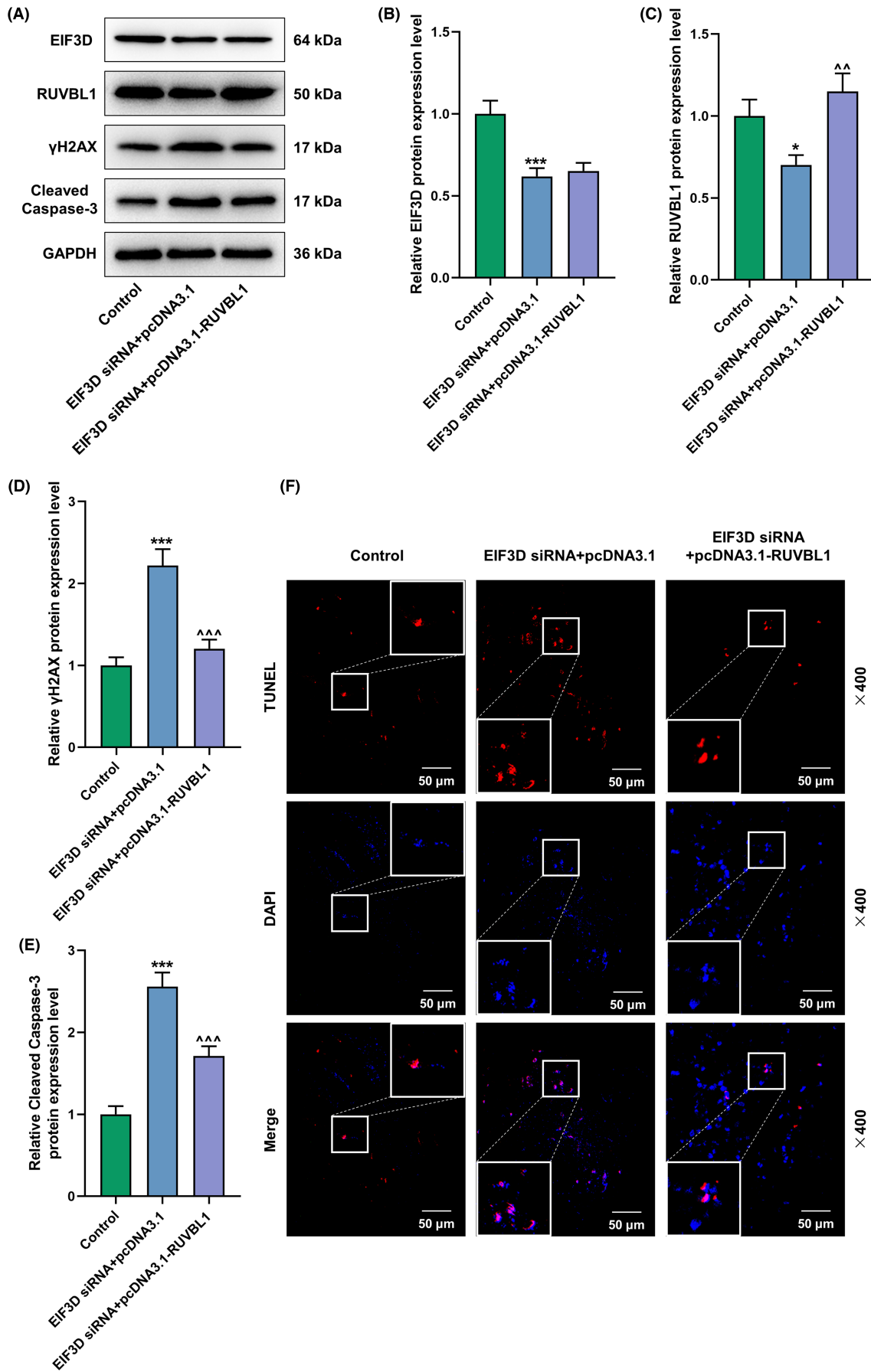


FIGURE 10 RUVBL1 overexpression reversed EIF3D silencing-caused promotion on γ H2AX expression and apoptosis in 5-Fu-treated mice. (A/B/C/D/E) The expressions of EIF3D, RUVBL1, γ H2AX, and Cleaved Caspase-3 in the murine xenograft tumors formed by SW480 cells co-transfected with EIF3D siRNA and RUVBL1 overexpression plasmids/the empty vector from 5-Fu (30 mg/kg)-treated mice were analyzed by Western blot, with GAPDH serving as the internal control. (F) The apoptosis of the murine xenograft tumors formed by SW480 cells co-transfected with EIF3D siRNA and RUVBL1 overexpression plasmids/the empty vector from 5-Fu (30 mg/kg)-treated mice was assessed by TUNEL staining. * $p < 0.05$; ^^ $p < 0.01$; *** p or ^^^ $p < 0.001$; * versus Control; * versus EIF3D siRNA+pcDNA3.1 (CRC, colorectal cancer; 5-Fu, 5-fluorouracil; EIF3D, eukaryotic translation initiation factor 3D; EIF3D siRNA, Small interfering RNA targeting EIF3D; RUVBL1, RuvB-like protein 1; pcDNA3.1-RUVBL1, RUVBL1 overexpression plasmids; GAPDH, glyceraldehyde 3-phosphate dehydrogenase; TUNEL, terminal deoxynucleotidyl transferase biotin-dUTP nick end labeling).

silencing-caused suppression of tumor growth, upregulation of γ H2AX, and promotion of apoptosis, as reflected by increased Cleaved Caspase-3 level and TUNEL-positivity in 5-Fu-treated mice, were attenuated by RUVBL1 overexpression. Meanwhile, notably, RUVBL1 overexpression could only cause a subtle (hardly discerned) reversion of EIF3D silencing-mediated EIF3D downregulation in the xenograft tumors of 5-Fu-treated mice. Thus, we confirmed that RUVBL1 upregulation plays a dominant role in EIF3D-caused 5-Fu resistance. However, our study is performed just in nonresistant CRC cells. To more effectively validate the 5-Fu-resistant mechanism of EIF3D, related experiments with 5-Fu-resistant CRC cells should be conducted in the future study. In addition, more clinical samples need to be further analyzed.

In conclusion, this study reveals that EIF3D upregulates RUVBL1 level by facilitating the specialized translation of RUVBL1, thus causing resistance to 5-Fu in CRC, which offers a novel anti-drug resistance strategy that may help bring promising results to the treatment of patients with advanced CRC.

CONFLICT OF INTEREST

The authors declare no conflicts of interest.

DATA AVAILABILITY STATEMENT

The analyzed data sets generated during the study are available from the corresponding author on reasonable request.

ORCID

Kemei Lu  <https://orcid.org/0000-0002-1499-7070>

REFERENCES

- Cunningham D, Atkin W, Lenz HJ, et al. Colorectal cancer. *Lancet*. 2010;375(9719):1030-1047.
- Watson AJ, Collins PD. Colon cancer: a civilization disorder. *Dig Dis*. 2011;29(2):222-228.
- Bray F, Ferlay J, Soerjomataram I, Siegel RL, Torre LA, Jemal A. Global cancer statistics 2018: GLOBOCAN estimates of incidence and mortality worldwide for 36 cancers in 185 countries. *CA Cancer J Clin*. 2018;68(6):394-424.
- Johdi NA, Sukor NF. Colorectal cancer immunotherapy: options and strategies. *Front Immunol*. 2020;11:1624.
- Allen KT, Chin-Sinex H, DeLuca T, et al. Dichloroacetate alters Warburg metabolism, inhibits cell growth, and increases the X-ray sensitivity of human A549 and H1299 NSC lung cancer cells. *Free Radic Biol Med*. 2015;89:263-273.
- Garg MB, Lincz LF, Adler K, Scorgie FE, Ackland SP, Sakoff JA. Predicting 5-fluorouracil toxicity in colorectal cancer patients from peripheral blood cell telomere length: a multivariate analysis. *Br J Cancer*. 2012;107(9):1525-1533.
- González-Perera I, Gutiérrez-Nicolás F, Nazco-Casariago GJ, et al. 5-fluorouracil toxicity in the treatment of colon cancer associated with the genetic polymorphism 2846 a>G (rs67376798). *J Oncol Pharm Pract*. 2017;23(5):396-398.
- Blondy S, David V, Verdier M, Mathonnet M, Perraud A, Christou N. 5-fluorouracil resistance mechanisms in colorectal cancer: from classical pathways to promising processes. *Cancer Sci*. 2020;111(9):3142-3154.
- Zheng Z, Li J, He X, et al. Involvement of RhoGDI2 in the resistance of colon cancer cells to 5-fluorouracil. *Hepatogastroenterology*. 2010;57(102-103):1106-1112.
- Shao J, Xu Y, Li H, et al. LMCD1 antisense RNA 1 (LMCD1-AS1) potentiates thyroid cancer cell growth and stemness via a positive feedback loop of LMCD1-AS1/miR-1287-5p/GLI2. *Ann Transl Med*. 2020;8(22):1508.
- Pestova TV, Kolupaeva VG. The roles of individual eukaryotic translation initiation factors in ribosomal scanning and initiation codon selection. *Genes Dev*. 2002;16(22):2906-2922.
- Algire MA, Maag D, Lorsch JR. Pi release from eIF2, not GTP hydrolysis, is the step controlled by start-site selection during eukaryotic translation initiation. *Mol Cell*. 2005;20(2):251-262.
- Hinnebusch AG. eIF3: a versatile scaffold for translation initiation complexes. *Trends Biochem Sci*. 2006;31(10):553-562.
- Zhang F, Xiang S, Cao Y, et al. EIF3D promotes gallbladder cancer development by stabilizing GRK2 kinase and activating PI3K-AKT signaling pathway. *Cell Death Dis*. 2017;8(6):e2868.
- Latosinska A, Mokou M, Makridakis M, et al. Proteomics analysis of bladder cancer invasion: targeting EIF3D for therapeutic intervention. *Oncotarget*. 2017;8(41):69435-69455.
- Fan Y, Guo Y. Knockdown of eIF3D inhibits breast cancer cell proliferation and invasion through suppressing the Wnt/ β -catenin signaling pathway. *Int J Clin Exp Pathol*. 2015;8(9):10420-10427.
- Gao Y, Teng J, Hong Y, et al. The oncogenic role of EIF3D is associated with increased cell cycle progression and motility in prostate cancer. *Med Oncol*. 2015;32(7):518.
- Lin Z, Xiong L, Lin Q. Correction to: expression of concern: knockdown of eIF3d inhibits cell proliferation through G2/M phase arrest in non-small cell lung cancer. *Med Oncol*. 2019;36(6):53.
- Du W, Cheng H, Peng L, Yang D, Yang C. hmiR-34c-3p upregulation inhibits the proliferation of colon cancer cells by targeting EIF3D. *Anticancer Drugs*. 2018;29(10):975-982.
- Huang H, Gao Y, Liu A, et al. EIF3D promotes sunitinib resistance of renal cell carcinoma by interacting with GRP78 and inhibiting its degradation. *EBioMedicine*. 2019;49:189-201.
- Sonenberg N. eIF4E, the mRNA cap-binding protein: from basic discovery to translational research. *Biochem Cell Biol*. 2008;86(2):178-183.
- Sonenberg N, Morgan MA, Merrick WC, Shatkin AJ. A polypeptide in eukaryotic initiation factors that crosslinks specifically to the 5'-terminal cap in mRNA. *Proc Natl Acad Sci U S A*. 1978;75(10):4843-4847.
- Leppke K, Das R, Barna M. Functional 5' UTR mRNA structures in eukaryotic translation regulation and how to find them. *Nat Rev Mol Cell Biol*. 2018;19(3):158-174.

24. Hsieh AC, Liu Y, Edlind MP, et al. The translational landscape of mTOR signalling steers cancer initiation and metastasis. *Nature*. 2012;485(7396):55-61.
25. Thoreen CC, Chantranupong L, Keys HR, Wang T, Gray NS, Sabatini DM. A unifying model for mTORC1-mediated regulation of mRNA translation. *Nature*. 2012;485(7396):109-113.
26. Gandin V, Masvidal L, Hulea L, et al. nanoCAGE reveals 5' UTR features that define specific modes of translation of functionally related MTOR-sensitive mRNAs. *Genome Res*. 2016;26(5):636-648.
27. Lee AS, Kranzusch PJ, Doudna JA, Cate JH. eIF3d is an mRNA cap-binding protein that is required for specialized translation initiation. *Nature*. 2016;536(7614):96-99.
28. Rowsell HC. The Canadian council on animal care—its guidelines and policy directives: the veterinarian's responsibility. *Can J Vet Res*. 1991;55(3):205.
29. Xu F, Ye ML, Zhang YP, et al. MicroRNA-375-3p enhances chemosensitivity to 5-fluorouracil by targeting thymidylate synthase in colorectal cancer. *Cancer Sci*. 2020;111(5):1528-1541.
30. Livak KJ, Schmittgen TD. Analysis of relative gene expression data using real-time quantitative PCR and the 2(-Delta Delta C(T)) method. *Methods*. 2001;25(4):402-408.
31. Yao X, Tu Y, Xu Y, Guo Y, Yao F, Zhang X. Endoplasmic reticulum stress confers 5-fluorouracil resistance in breast cancer cell via the GRP78/OCT4/lncRNA MIAT/AKT pathway. *Am J Cancer Res*. 2020;10(3):838-855.
32. Yu X, Zheng B, Chai R. Lentivirus-mediated knockdown of eukaryotic translation initiation factor 3 subunit D inhibits proliferation of HCT116 colon cancer cells. *Biosci Rep*. 2014;34(6):e00161.
33. Ma Y, Miao Y, Peng Z, et al. Identification of mutations, gene expression changes and fusion transcripts by whole transcriptome RNAseq in docetaxel resistant prostate cancer cells. *SpringerPlus*. 2016;5(1):1861.
34. Van der Jeught K, Xu HC, Li YJ, Lu XB, Ji G. Drug resistance and new therapies in colorectal cancer. *World J Gastroenterol*. 2018;24(34):3834-3848.
35. Kim JH. Chemotherapy for colorectal cancer in the elderly. *World J Gastroenterol*. 2015;21(17):5158-5166.
36. Yan D, Tu L, Yuan H, et al. WBSCR22 confers oxaliplatin resistance in human colorectal cancer. *Sci Rep*. 2017;7(1):15443.
37. Morawska K, Goirand F, Marceau L, et al. 5-FU therapeutic drug monitoring as a valuable option to reduce toxicity in patients with gastrointestinal cancer. *Oncotarget*. 2018;9(14):11559-11571.
38. Shibata J, Aiba K, Shibata H, Minowa S, Horikoshi N. Detection and quantitation of thymidylate synthase mRNA in human colon adenocarcinoma cell line resistant to 5-fluorouracil by competitive PCR. *Anticancer Res*. 1998;18(3a):1457-1463.
39. Elmore S. Apoptosis: a review of programmed cell death. *Toxicol Pathol*. 2007;35(4):495-516.
40. He Z, Gharaibeh RZ, Newsome RC, et al. *Campylobacter jejuni* promotes colorectal tumorigenesis through the action of cytolethal distending toxin. *Gut*. 2019;68(2):289-300.
41. Lauscher JC, Loddenkemper C, Kosel L, Gröne J, Buhr HJ, Huber O. Increased pontin expression in human colorectal cancer tissue. *Hum Pathol*. 2007;38(7):978-985.
42. Kanemaki M, Makino Y, Yoshida T, et al. Molecular cloning of a rat 49-kDa TBP-interacting protein (TIP49) that is highly homologous to the bacterial RuvB. *Biochem Biophys Res Commun*. 1997;235(1):64-68.
43. Fan W, Xie J, Xia J, et al. RUVBL1-ITFG1 interaction is required for collective invasion in breast cancer. *Biochim Biophys Acta Gen Subj*. 2017;1861(7):1788-1800.
44. Guo H, Zhang XY, Peng J, et al. RUVBL1, a novel C-RAF-binding protein, activates the RAF/MEK/ERK pathway to promote lung cancer tumorigenesis. *Biochem Biophys Res Commun*. 2018;498(4):932-939.
45. Lin D, Lin B, Bhanot H, et al. RUVBL1 is an amplified epigenetic factor promoting proliferation and inhibiting differentiation program in head and neck squamous cancers. *Oral Oncol*. 2020;111:104930.
46. Assimon VA, Tang Y, Vargas JD, et al. CB-6644 is a selective inhibitor of the RUVBL1/2 complex with anticancer activity. *ACS Chem Biol*. 2019;14(2):236-244.
47. Li H, Zhou T, Zhang Y, Jiang H, Zhang J, Hua Z. RuvBL1 maintains resistance to TRAIL-induced apoptosis by suppressing c-Jun/AP-1 activity in non-small cell lung cancer. *Front Oncol*. 2021;11:679243.

SUPPORTING INFORMATION

Additional supporting information can be found online in the Supporting Information section at the end of this article.

How to cite this article: Li C, Lu K, Yang C, Du W, Liang Z. EIF3D promotes resistance to 5-fluorouracil in colorectal cancer through upregulating RUVBL1. *J Clin Lab Anal*. 2023;37:e24825. doi:[10.1002/jcla.24825](https://doi.org/10.1002/jcla.24825)